

MODELING OF GAMMA-RAY MILLISECOND PULSAR LIGHT CURVES REVEALED BY *FERMI*-LAT

C. VENTER^{1,2,3}, A. K. HARDING¹, and L. GUILLEMOT⁴

¹*Astrophysics Science Division, NASA Goddard Space Flight Center, Greenbelt, MD 20771, USA*

²*Unit for Space Physics, North-West University, Potchefstroom Campus, Private Bag X6001,
Potchefstroom 2520, South Africa*

³*NASA Postdoctoral Program Fellow*

⁴*CNRS/IN2P3, Université de Bordeaux, Centre d'Études Nucléaires de Bordeaux Gradignan,
UMR 5797, 33175 Gradignan, France*

Fermi Large Area Telescope (LAT) has recently detected 8 gamma-ray millisecond pulsars (MSPs), providing an unprecedented opportunity to probe the magnetospheres of these low-spin-down pulsars. We performed 3D emission modeling, including various Special Relativistic effects, in the context of pair-starved polar cap (PSPC), slot gap (SG), and outer gap (OG) pulsar models. Most of the light curves are best fit by SG and OG models, surprisingly indicating the presence of narrow accelerating gaps limited by robust pair production. All model fits imply high-altitude emission, and we observe exclusive differentiation of the current gamma-ray MSP population into two sub-classes: light curve shapes and lags across wavebands impose either PSPC or SG / OG-type geometries.

1 Introduction

Millisecond pulsars (MSPs) are rapidly-rotating neutron stars, characterized by relatively short spin periods and low surface magnetic fields. It is thought that transfer of mass and angular momentum from a binary companion during an accretion phase, may revive their “dead” (radio-invisible) younger pulsar progenitors which have “spun down” previously.¹ MSPs are thus believed to be “recycled” pulsars,² descending from low-mass X-ray binaries (LMXBs).³

MSPs were predicted to be visible in gamma rays.^{4,5,6,7,8,9,10} Observational confirmation was provided by the *Fermi* Large Area Telescope (LAT), a high-energy (HE) gamma-ray telescope with a large field of view (2.4 sr), operating in the energy range ~ 20 MeV to > 300 GeV¹¹, which recently detected 8 gamma-ray MSPs.¹²

Mainly two different models have been employed to describe HE radiation from pulsars. Polar cap (PC) models¹³ assume injection of primary electrons from the stellar surface. These primaries radiate HE curvature radiation (CR) or inverse Compton scattering (ICS) gamma rays which are converted into electron-positron pairs via magnetic pair production. A low-altitude pair formation front (PFF) is established close to the surface, screening the accelerating electric field.¹⁴ By allowing variation of the CR PFF altitude across the PC, a slot gap (SG) is formed along the last open magnetic field lines. This gap extends from the neutron star surface to near the so-called light cylinder, and allows acceleration of primaries up to high altitudes.^{15,16} The SG model is a possible physical realization of the two-pole caustic geometry.¹⁷ Outer gap (OG) models^{18,19,20} assume that HE radiation is generated by cascades of electron-positron pairs

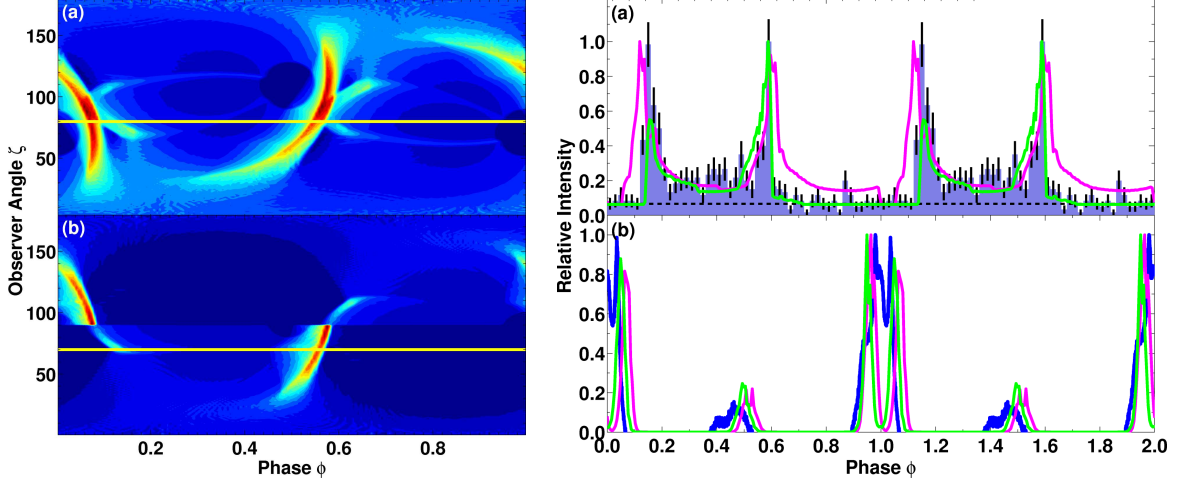


Figure 1: *Left*: Phaseplots for PSR J0030+0451. Panel (a) is for an SG model with $(\alpha, \zeta) = (70^\circ, 80^\circ)$, while panel (b) is for an OG model with $(\alpha, \zeta) = (80^\circ, 70^\circ)$. *Right*: Observed and fitted light curves for PSR J0030+0451. In panel (a), we show the *Fermi*-LAT data (histogram) with estimated background level (dashed line), and SG (magenta line) and OG (green line) fits. Panel (b) shows the radio data (blue line), and the magenta and green lines correspond to the same (α, ζ) combinations as those of the SG and OG fits in panel (a).

produced via photon-photon pair creation. This emission occurs close to the last open field lines, above the “null-charge surface”, and is thus confined to the outer magnetosphere. Recently, a 3D OG solution was found²¹ which extends toward the NS surface. For MSPs with mostly unscreened magnetospheres, a “pair-starved polar cap” (PSPC) model^{22,10} applies in which charges are accelerated up to high altitudes over the full open-field-line region.

We study the *Fermi*-LAT MSP population¹² using 3D emission modeling, including Special Relativistic (SR) effects of aberration and time-of-flight delays, and rotational sweepback of B-field lines,^{23,24,25} in the context of geometric SG and OG models, as well as a CR PSPC model, and obtain fits for gamma-ray and radio light curves. Our calculations are complementary to another study⁹ that focuses on younger pulsars. More details are provided elsewhere.¹⁰

2 Model Description

We use an implementation^{26,27} of the retarded vacuum dipolar B-field solution²⁸ of a rotator inclined by an angle α with respect to the rotation axis. The PC shape is distorted asymmetrically by rotational sweepback of field lines. We calculate the curvature radius of the B-field lines in the inertial observer frame, and assume SG and OG gaps to be confined between two field lines with footpoints close to the PC rim, and having constant emissivity over the emitting volume. In the PSPC case, we collect photons with energies above 100 MeV from the full open-field-line region.

For the PSPC regime, we only consider CR losses suffered by electron primaries moving along the field lines. Previous studies^{4,5,7,8,29} have used lower-altitude solutions^{14,30} for E_{\parallel} , the PSPC E-field parallel to the B-field. As *Fermi*-LAT results seem to indicate that the HE radiation is originating in the outer magnetosphere,¹² we now incorporate the solution²² for altitudes close to the light cylinder in the small-angle approximation by matching this solution to the two lower-altitude ones. We find conservation of energy when solving the transport equation for relativistic electron primaries using the full E-field solution.

We use an empirical radio cone model based on the characterization³¹ of the radio emission as magnetic axis-centered core and conal beams. We adopt a description³² based on fits³³ of average-pulse profiles of a small collection of pulsars at 400 MHz. The conal emission occurs

Table 1: Model fits for inclination and observer angles α , ζ .

Name	α_{SG} ($^{\circ}$)	ζ_{SG} ($^{\circ}$)	α_{OG} ($^{\circ}$)	ζ_{OG} ($^{\circ}$)	α_{PSPC} ($^{\circ}$)	ζ_{PSPC} ($^{\circ}$)	α_{radio} ($^{\circ}$)	ζ_{radio} ($^{\circ}$)
J0030+0451	70	80	80	70			~ 62	~ 72
J0218+4232	60	60	50	70			~ 8	~ 90
J0437-4715	30	60	30	60			20 – 35	16 – 20
J0613-0200	30	60	30	60			small ($\zeta - \alpha$)	
J0751+1807	50	50	50	50				
J1614-2230	40	80	40	80				
J1744-1134					50	80		
J2124-3358					40	80	20 – 60 (48)	27 – 80 (67)

at altitudes of 10% – 20% of the light cylinder radius. We lastly use relative units for the cone beam luminosity.

3 Results

SR effects of aberration and time-of-flight delays cause phase shifts that nearly cancel those due to the curvature of the B-field on trailing field lines, leading to accumulation of emission (initially emitted tangentially to the B-field lines) around narrow phase bands ϕ . This results in caustic structures (on phaseplots of ζ vs. ϕ , with ζ the observer angle) around $\phi \sim 0.0 - 0.1$ and $\phi \sim 0.4 - 0.6$ in phase for SG and OG models. No emission originates below the null charge surface in the OG model, so that an observer can only see emission from one magnetic pole, in contrast to the SG models.

We studied a large number of light curves for each of the different pulsar models. Both OG and SG models have a preponderance of double-peaked light curves at similar phases. OG models do not exist at all angle combinations, while SG models do (due to emission occurring below the null charge surface). One may find sharp, solitary peaks for some regions in (α, ζ) -space in OG models, while the corresponding SG-peaks usually have additional low-level features. The PSPC model have mostly single-peaked gamma-ray profiles roughly in phase with the (single) radio peaks, but one may see radiation from both poles for large α , leading to double-peaked profiles separated by ~ 0.5 in phase. The radio peak multiplicity depends on the observer’s geometry. In significantly off-beam geometries, only the relatively larger gamma-ray cone is seen, explaining the phenomenon of “radio-quiet” pulsars.

We chose best-fit light curves from the various models to match the MSP gamma-ray and radio data by eye. As an example, the left panel of Figure 1 shows phaseplots associated with the best light curve fits (right panel) obtained for PSR J0030+0451. We inferred values for α and ζ for each MSP (Table 1), and compared them with (somewhat uncertain) values obtained from radio polarimetric measurements (references for radio data elsewhere¹⁰).

4 Discussion and Conclusions

We have compared 3D model predictions of gamma-ray and radio radiation with MSP gamma-ray data from *Fermi*-LAT in the framework of geometric SG and OG pulsar models, and also for the full-radiation PSPC model. Surprisingly, some MSPs have double-peaked light curves well fit by SG / OG models, indicating strong screening of E_{\parallel} by pair production. The larger radio beam widths of MSPs compared to those of canonical pulsars furthermore implies relatively few

radio-quiet MSPs. We found exclusive differentiation between the SG / OG models on the one hand, and the PSPC model on the other hand. Emission in *all* models considered comes from the outer magnetosphere. Our fits of α and ζ are in reasonable agreement with values inferred from MSP radio polarization measurements. For PSR J0437-4715 and PSR J0613-0200, the SG model predicts a small precursor to the main gamma-ray peak, but not the OG model. This may become a future model discriminator. Future phase-resolved spectroscopy made possible by the quality of *Fermi*-LAT data should challenge pulsar models.

Acknowledgments

CV is supported by the NPP at the Goddard Space Flight Center, administered by ORAU through a contract with NASA, and also by the South African National Research Foundation. AKH acknowledges support from the NASA Astrophysics Theory Program.

References

1. M.A. Alpar *et al.*, *Nature* **300**, 728 (1982)
2. D. Bhattacharya, D., and E.P.J. van den Heuvel, *Phys. Rep.* **203**, 1 (1991)
3. A.M. Archibald *et al.*, *Science* **324**, 1411 (2009)
4. A.K. Harding, V.V. Usov, and A.G. Muslimov, *ApJ* **622**, 531 (2005)
5. M. Frackowiak, and B. Rudak, *Adv. Space Res.* **35**, 1152 (2005a)
6. L. Zhang, J. Fang, and S.B. Chen, *ApJ* **666**, 1165 (2007)
7. C. Venter, O.C. de Jager, and A.-C. Clapson, *ApJL* **696**, L52 (2009)
8. A. Zajczyk, astro-ph:0805.2505 (2008)
9. K.P. Watters, R.W. Romani, P. Weltevrede, and S. Johnston, *ApJ* **695**, 1289 (2009)
10. C. Venter, A.K. Harding, and L. Guillemot, submitted to *ApJ* (2009)
11. W.B. Atwood *et al.*, *ApJ* **697**, 1071 (2009)
12. A.A. Abdo *et al.* (for the *Fermi-LAT* Collaboration), *Science* **325**, 848 (2009)
13. J.K. Daugherty, and A.K. Harding, *ApJ* **458**, 278 (1996)
14. A.K. Harding, and A.G. Muslimov, *ApJ* **508**, 328 (1998)
15. J. Arons, *ApJ* **266**, 215 (1983)
16. A.G. Muslimov, and A.K. Harding, *ApJ* **606**, 1143 (2004a)
17. J. Dyks, and B. Rudak, *ApJ* **598**, 1201 (2003)
18. K.S. Cheng, C. Ho, and M. Ruderman, *ApJ* **300**, 500 (1986a)
19. K.S. Cheng, C. Ho, and M. Ruderman, *ApJ* **300**, 522 (1986b)
20. R.W. Romani, *ApJ* **470**, 469 (1996)
21. K. Hirotani, submitted to the *Open Astronomy Journal*, astro-ph:0809.1283 (2008)
22. A.G. Muslimov, and A.K. Harding, *ApJ* **617**, 471 (2004b)
23. M. Morini, *MNRAS* **202**, 495 (1983)
24. R.W. Romani, and I.-A. Yadigaroglu, *ApJ* **438**, 314 (1995)
25. J. Dyks, B. Rudak, and A.K. Harding, *ApJ* **607**, 939 (2004)
26. J. Dyks, and A.K. Harding, *ApJ* **606**, 1125 (2004a)
27. J. Dyks, and A.K. Harding, *ApJ* **614**, 869 (2004b)
28. A. J. Deutsch, *Ann. d’Astrophys.* **18**, 1 (1955)
29. C. Venter, and O.C. de Jager, *ApJ* **619**, L167 (2005)
30. A.G. Muslimov, and A.K. Harding, *ApJ* **485**, 735 (1997)
31. J.M. Rankin, *ApJ* **405**, 285 (1993)
32. P.L. Gonthier, R. van Guilder, and A.K. Harding, *ApJ* **604**, 775 (2004)
33. Z. Arzoumanian, D.F. Chernoff, and J.M. Cordes, *ApJ* **568**, 289 (2002)